

## CHAPTER 1

# Introduction to Aluminum-Silicon Casting Alloys

COMMERCIAL CAST ALUMINUM-SILICON alloys are polyphase materials of composed microstructure belonging to the Aluminum Association classification series 3xx.x for aluminum-silicon plus copper and/or magnesium alloys and 4xx.x aluminum-silicon alloys. They are designated by standards such as CEN EN 1706, “Aluminum and Aluminum Alloys. Castings. Chemical Composition and Mechanical Properties,” and are designated in ASTM standards according to the method of casting:

- ASTM B 26/B 26M, “Specification for Aluminum-Alloy Sand Casting”
- ASTM B 85, “Specification for Aluminum-Alloy Die Casting”
- ASTM B 108, “Specification for Aluminum-Alloy Permanent Mold Casting”

Their use as structural materials is determined by their physical properties (primarily influenced by their chemical composition) and their mechanical properties (influenced by chemical composition and microstructure).

The characteristic property of aluminum alloys is relatively high tensile strength in relation to density (Table 1.1) compared with that of other cast alloys, such as ductile cast iron or cast steel. The high specific tensile strength of aluminum alloys is very strongly influenced by their composed polyphase microstructure.

The silicon content in standardized commercial cast aluminum-silicon alloys is in the range of 5 to 23 wt%. The structure of the

alloys can be hypoeutectic, hypereutectic, or eutectic, as can be seen on the equilibrium phase diagram (Fig. 1.1a). The properties of a specific alloy can be attributed to the individual physical properties of its main phase components ( $\alpha$ -aluminum solid solution and silicon crystals) and to the volume fraction and morphology of these components.

### 1.1 Properties of $\alpha$ -Aluminum Solid Solution

The  $\alpha$ -aluminum solid solution is the matrix of cast aluminum-silicon. It crystallizes in the form of nonfaceted dendrites, on the basis of crystallographic lattice of aluminum. This is a face-centered cubic (fcc) lattice system, noted by the symbol A1, with coordination number of 12, and with four atoms in one elementary cell (Ref 1–3). Lattice A1 is one of the closest packed structures, with a very high filling factor of 0.74 (Fig. 1.2a). The plane of the closest filling is the plane {111}, and the direction  $\langle 110 \rangle$  is the closest filling direction in this lattice (Table 1.2). Atoms are connected with metallic bonds characterized by isotropy and relatively low bonding energy (Ref 1, 2, 8). Each aluminum atom gives three valence electrons to an electron gas, filling the spaces among the nodes of the crystallographic lattice, formed by aluminum ions (Fig. 1.2b). Under external loading these ions can change their relative position in the lattice in some range, without breaking the interatomic bonds (Ref 1). The plastic deformation of crystals of metallic bonds is the macroscopic effect of this relative displacement of ions in nodes of their lattice. The breaking of the continuity of interatomic bonds in the ideal crystal takes place when the external stress exceeds the cohesive force value in the crystallographic planes (Ref 4–7). The value of this critical stress, estimated in Eq 1.1, is equal to  $E/10$  (Ref 4):

$$\sigma_{\max} = (2E\Gamma_s/\pi b)^{1/2} \quad (\text{Eq 1.1})$$

where  $\sigma_{\max}$  is the stress along axis perpendicular to crystallographic plane, in which the interatomic bonds are broken,  $E$  is the elastic modulus,  $\Gamma$  is the surface free energy, and  $b$  is the atomic diameter.

The value of this material constant is directly dependent on the physical properties of the crystallographic lattice and the atom

**Table 1.1 Mechanical properties of selected cast engineering materials**

Alloy	Ultimate tensile strength (UTS), MPa	Density ( $\rho$ ), kg/m <sup>3</sup>	Specific strength (UTS/ $\rho$ ), m <sup>2</sup> /s <sup>2</sup>
Pure Al (99.9999% Al) Al (4N)	78	2699	0.03
Al-7%Si, T6	210	2685	0.09
Al-5%Si-2%Cu, T6	310	2690	0.12
Al-9%Si, T6	240	2650	0.10
Al-20%Si, T6	200	2650	0.08
Iron	1.9	7650	0.00024
Gray cast iron	380	7100	0.05
Ductile cast iron	900	7200	0.13
Austempered ductile cast iron	1200	7200	0.17
Cast carbon steel	650	7850	0.08
Cast stainless steel	880	7850	0.11

size. On the basis of several different fracture models, it has been determined that the  $\sigma_{\max}$  value can be in the range of  $E/4$  to  $E/15$  (Ref 5). The value of  $\sigma_{\max}$  is called the theoretical tensile strength of ideal crystal. This value is several times greater than the tensile strength estimated experimentally for the real crystals or polycrystalline materials (Table 1.3). The tensile strength of the whisk-

ker crystals of aluminum can be compared to the theoretical one (their tensile strength is only 6.6 times less than theoretical one).

Theoretical proof stress—defined as the stress causing the permanent plastic deformation of crystallographic lattice (critical tangent stress  $\tau_{\max}$  on slip plane,  $\tau_{\max} = G/2$ , where  $G$  is shear modulus)—is  $10^4$  times higher than the value estimated experimentally

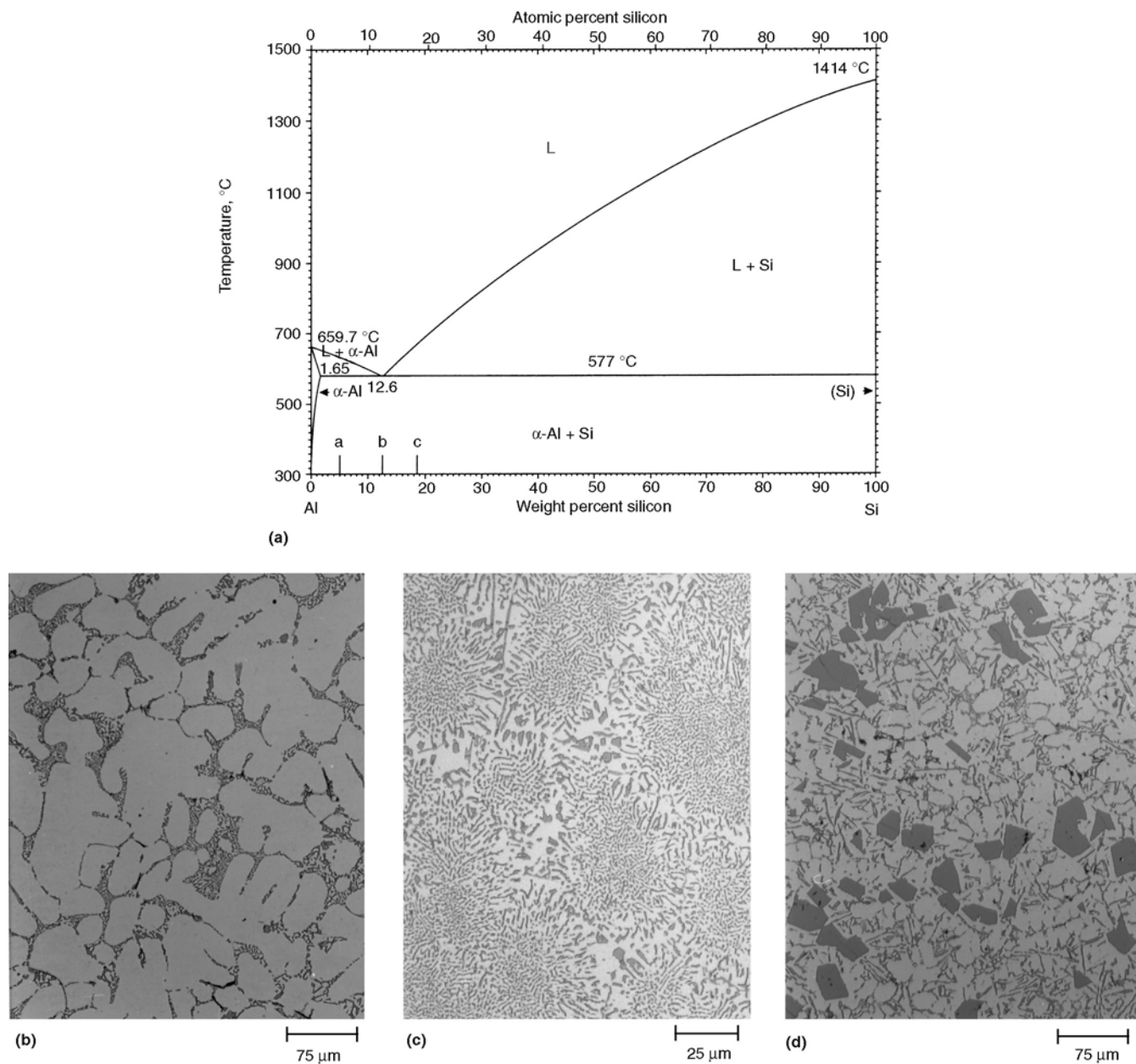


**Fig. 1.1** Commercial cast aluminum-silicon alloys. (a) Al-Si equilibrium diagram. (b) Microstructure of hypoeutectic alloy (1.65-12.6 wt% Si). 150X. (c) Microstructure of eutectic alloy (12.6% Si). 400X. (d) Microstructure of hypereutectic alloy (>12.6% Si). 150X

**Table 1.2** Parameters of the elementary cells of A1 and A4 crystal lattice

Element	Lattice type	Unit cell dimension, nm	Coordination number	Number of atoms in the unit cell	Filling factor	Bonding energy, kJ/mol (Ref 1)
Al	A1	0.40333	12	4	0.74	105–837
Si	A4	0.543035	4	8	0.34	523–1255

(Ref 5, 6). The reason for such comparatively low tensile strength in the real crystallographic lattice is due to the presence of defects, such as point defects (vacancies), line defects (dislocations), and surface defects (stacking faults).

The stacking-fault energy of crystallographic lattice of aluminum is very high, and very high density of moving dislocations (Ref 5, 6) is present. In Al (fcc) metals, the Peierls-Nabarro (P-N) forces—that is, the resistance to dislocation movement—are low and almost do not affect the proof stress value. Their effect becomes quite noticeable at the liquid nitrogen temperature,  $-196^{\circ}\text{C}$  ( $-321^{\circ}\text{F}$ ) (Ref 5, 6).

The slip, causing permanent plastic deformation, is relatively easy, because in the Al lattice there are 12 systems of easy slip:  $\{111\}$ ,  $\langle 110 \rangle$ . The plane  $\{111\}$  of the smallest surface energy is an energy-privileged plane of the easy slip. The small distance between partial dislocations makes their recombination easy, and the wave type transverse slip (of wavy glide type) can take place

as well (Ref 6). The features of the real Al lattice, mentioned above, cause the low resistance to deformation. It can be estimated from an empirical formula (Ref 6):

$$\sigma = k\varepsilon^n \quad (\text{Eq 1.2})$$

where  $\sigma$  is real stress,  $\varepsilon$  is real strain,  $k$  is the strain-hardening factor, and  $n$  is a material constant.

The strain-hardening factor in Eq 1.2 for aluminum is 0.15 to 0.25, which is about half that of copper, bronze, or austenitic steel (Ref 6).

## 1.2 Properties of Silicon Crystals

The silicon precipitates, present in commercial aluminum-silicon alloys, are almost pure, faceted crystals of this element (Fig. 1.3). They can have different morphology: primary, compact, massive precipitates in hypereutectic alloy or branched plates in aluminum-silicon eutectic (Ref 10–13).

Silicon crystal lattice is A4, cubic, of diamond type. Each atom is bonded with four others with covalent bonds, forming a tetrahedron. Eight tetrahedrons form one elementary cell of A4 lattice,

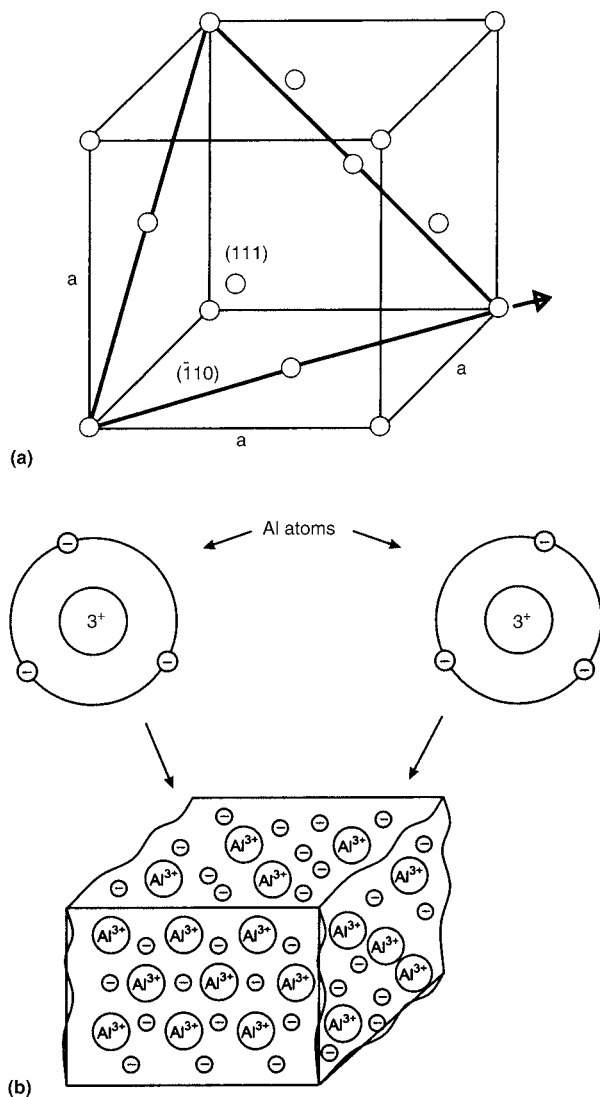


**Fig. 1.2** Crystal structure of aluminum. (a) Elementary cell of a cubic crystalline lattice Al. (b) Aluminum atoms with outer electrons that develop the interatomic bonds in lattice Al. Source: Ref 1

**Table 1.3** Mechanical properties of aluminum and silicon crystals

Property	Al	Si
Peierls-Nabarro forces	Small	Big
Stacking fault energy	Big 250 mJ/m <sup>2</sup> (a) 200 mJ/mol(b)	Small
Slip system	$\{111\}$ ; $\langle 110 \rangle$ (a)(c)	$\{111\}$ ; $\langle 1\bar{1}0 \rangle$ (a)
Strain-hardening factor	0.15–0.25(a)	...
Shear modulus ( $G$ ) of monocrystal, GPa	26.7(d)(e) 29(c)	...
Shear modulus ( $G$ ) of polycrystal, GPa	27.2(c)	40.5(c)
Theoretical yield strength (critical tangent stress on slip plane), GPa	4.26(e) 11.3(a)	6.4(c)
Experimental yield strength of monocrystal, MPa	0.78(d)(f)	...
Elastic modulus ( $E$ ) of monocrystal, GPa	$c_{11}$ , 108 $c_{12}$ , 62 $c_{44}$ , 28(g)	$c_{11}$ , 166 $c_{12}$ , 64 $c_{44}$ , 79(g)
Elastic modulus ( $E$ ) of whisker, GPa	506(c)	169(c)
Whisker tensile strength ( $R_m$ ), GPa	15.5(c)	6.6(c)
Elastic modulus ( $E$ ) of polycrystal, GPa	70(c) 71.9(c)	115(c)
Tensile strength of polycrystal, MPa	99.999% Al, 44.8(b) 99.99% Al, 45(h) 99.80% Al, 60(h)	5.3 GPa(c)
Hardness	99.999% Al, 120–140 HV(i)	1000–1200 HV(j) 8700–13500 N/m <sup>2</sup> (a)
Cleavage energy	...	$\{111\}$ , 890 mJ/m <sup>2</sup> (c)
Point defects hardening factor	$G/10$ for symmetric defects; $2G$ for nonsymmetric defects(a)	...

Source: (a) Ref 6. (b) Ref 1. (c) Ref 7. (d) Ref 8. (e) Ref 2. (f) Ref 5. (g) Ref 9. (h) Ref 3. (i) Ref 10. (j) Ref 11

face centered, with four additional atoms from the center of each tetrahedron. This structure is less close packed than Al lattice (Table 1.2). The filling factor is 0.34 (Ref 1, 8, 9). The neighboring atoms give four valence electrons and form a common hybrid orbital. The common, external shell circles the atoms in the lattice nodes and forms electron pairs of antiparallel spins (Fig. 1.4b) (Ref 2, 8). Characteristic features of the covalent bond are its high energy (523 to 1255 kJ/mol) and its anisotropy (Ref 1, 8, 9). Atoms, connected with covalent bonds, cannot displace under an external force until the bonds are completely broken. The material then

cracks instantly, and decohesion takes place on the cleavage planes. Microscopic observations showed that the cleavage plane is the preferential plane for the brittle fracture, because of its small surface energy. In silicon this is plane  $\{111\}$ . Cleavage work, necessary for breaking the atomic bonds in this plane, is equal to 890 J/m<sup>2</sup> (Ref 7). In crystals with covalent bonds, the density of dislocations is small, and P-N forces are high (Ref 1, 5, 6). This is the reason for the high proof stress of silicon and its inclination to brittle cracking. Its slip system, which can be active in silicon crystals, is  $\{111\} \langle \bar{1}10 \rangle$  (of planar glide type) (Ref 6).

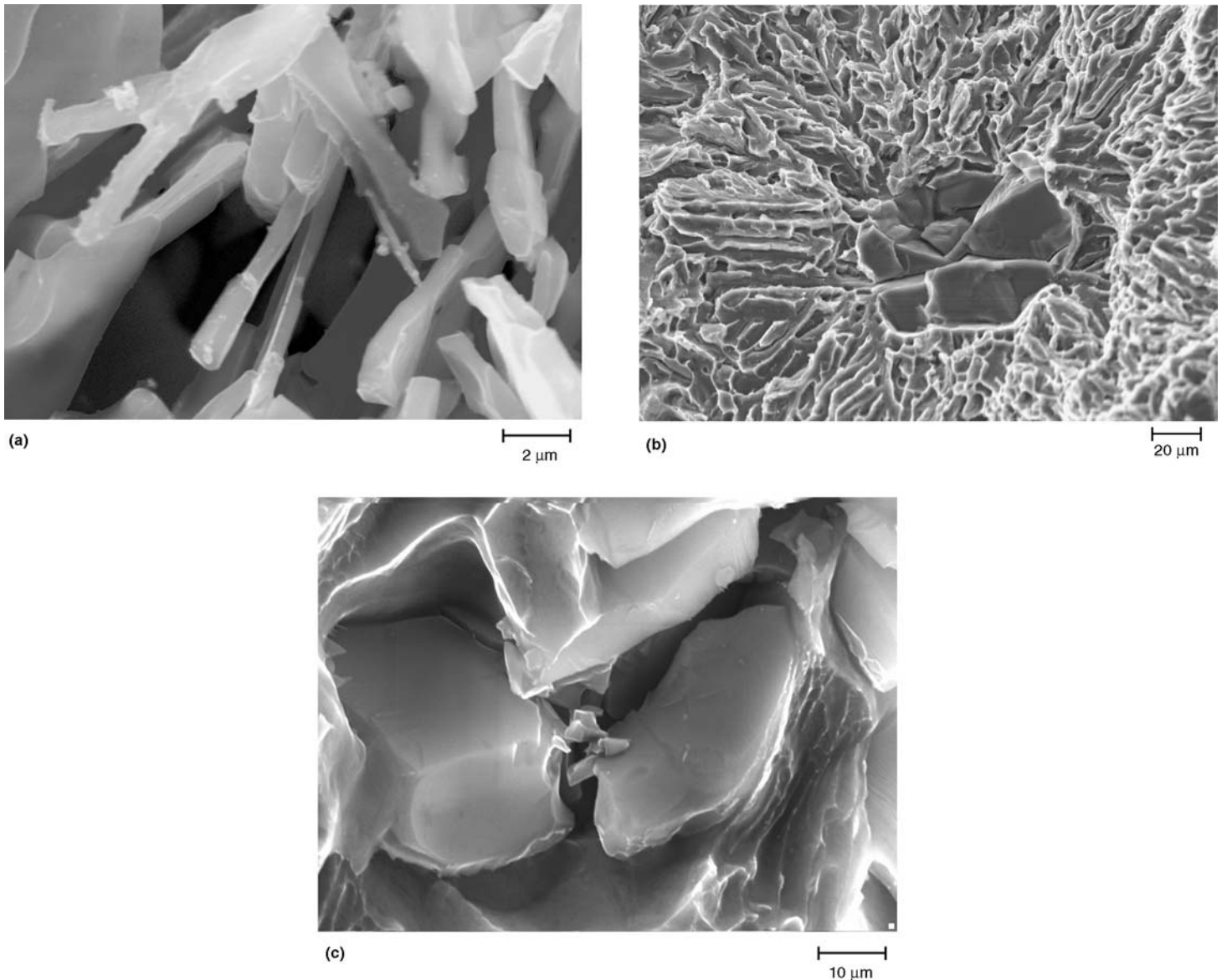


**Fig. 1.3** Morphology of the silicon crystals in aluminum-silicon alloys. (a) Silicon crystals in eutectic as-cast alloy. Scanning electron micrograph (SEM). 6500 $\times$ . (b) Primary silicon crystals in hypereutectic as-cast alloy. SEM. 400 $\times$ . (c) Silicon crystals in hypoeutectic alloy modified, after heat treatment. SEM. 1500 $\times$



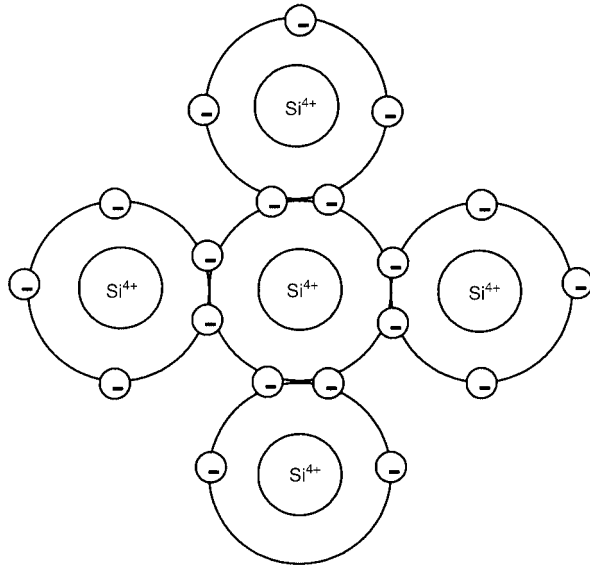
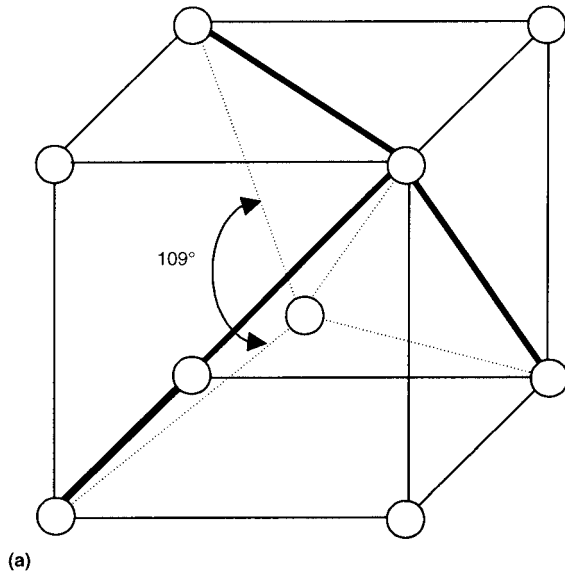


**Fig. 1.4** Crystal structure of silicon. (a) Elementary cell of the crystalline lattice silicon. (b) Interatomic bonds in lattice silicon. Source: Ref 1, 8, 9

### 1.3 Properties of Aluminum-Silicon Alloys

The simplest model of microstructure of cast aluminum-silicon alloys can be presented in the form shown in Fig. 1.5: a soft continuous matrix ( $\alpha$ -aluminum-solid solution) containing hard precipitates of silicon of different morphology.

Assuming an important simplification, the average stress in this material can be evaluated as a linear function of the volume fraction of silicon (Ref 7):

$$\sigma = \sigma_{\alpha} V_{\alpha}^{\alpha} + \sigma_{\text{Si}} V_{\text{Si}}^{\text{Si}} = \sigma_{\alpha} + V_{\text{Si}}^{\text{Si}} (\sigma_{\text{Si}} - \sigma_{\alpha}) \quad (\text{Eq 1.3})$$

where  $\sigma_{\alpha}$  and  $\sigma_{\text{Si}}$  are stresses in the volume unit.

The stress-intensity factor depends on the elastic and the plastic properties of the matrix and on the size of the brittle phase particles (Ref 14, 15). In Eq 1.3, the influence of the morphology, the average size, and the distribution of brittle particles, that is, silicon precipitates, are not taken into account. These microstructure parameters can differentiate the properties of materials of similar value of the silicon volume fraction to an important degree. In the polycrystalline material, the Hall-Petch equation can express the influence of the morphology of the microstructure constituents on the proof stress (Ref 1, 6, 7):

$$\sigma_{\text{pl}} = \sigma_s + k_m d^{-1/2} \quad (\text{Eq 1.4})$$

where  $\sigma_{\text{pl}}$  is the proof stress of the polycrystalline specimen,  $\sigma_s$  is the resistance of the lattice to dislocation movement,  $k_m$  is the hardening factor (effect of hardening by grain boundaries), and  $d$  is the grain diameter.

The stress  $\sigma_s$  can be divided into two parts:  $\sigma_d$  and  $\sigma_p$ .  $\sigma_d$  is independent of temperature but dependent on the structure of lattice, and it expresses interaction among dislocations, precipitates, and additional atoms.  $\sigma_p$  is temperature dependent and is connected with P-N stress value (Ref 6):

$$\sigma_{\text{pl}} = \sigma_p + \sigma_d + k_m d^{-1/2} \quad (\text{Eq 1.5})$$

where  $\sigma_p$  represents P-N stresses, a short-range effect ( $<1$  nm);  $\sigma_d$  is the dislocation stress field, a medium-range effect (10 to 100 nm); and  $k_m d^{-1/2}$  is the long-range effect ( $>1000$  nm). One can say that the influence of the degree of microstructure dispersion on the proof stress is a long-range effect.

Many published experimental examinations show that in case of dendrite structure materials the microstructure effect in the Hall-Petch formula is dependent on  $\lambda$ , the dendrite arm size, and  $\gamma$ , the size of silicon lamellas (Ref 16–20). Relationships between ultimate tensile strength ( $R_m$ ) and secondary dendrite arm size, evaluated experimentally for alloy C356, can be expressed by:

$$R_m = k + k_2 \gamma^{-1/2} + k_3 \lambda^{-1/2} \quad (\text{Eq 1.6})$$

$$R_{0.2} = k + k_5 \gamma^{-1/2} + k_6 \lambda^{-1/2} \quad (\text{Eq 1.7})$$

where  $k$ ,  $k_2$ ,  $k_3$ ,  $k_5$ , and  $k_6$  are empirical constants,  $\gamma$  is the size of silicon lamellas in interdendritic eutectic regions, and  $\lambda$  is the secondary dendrite arm size.  $R_{0.2}$  is the 0.2% proof strength.

The mechanical properties of cast aluminum-silicon alloys can be improved by cast technology and heat treatment processes that:

- Increase the strength of soft matrix
- Decrease the brittle fracture risk in the polyphase regions
- Increase the degree of dispersion of the dendritic structure

An increase in strength of soft matrix of  $\alpha$ -aluminum solid solution can be achieved by its hardening with point defects, such as sub-

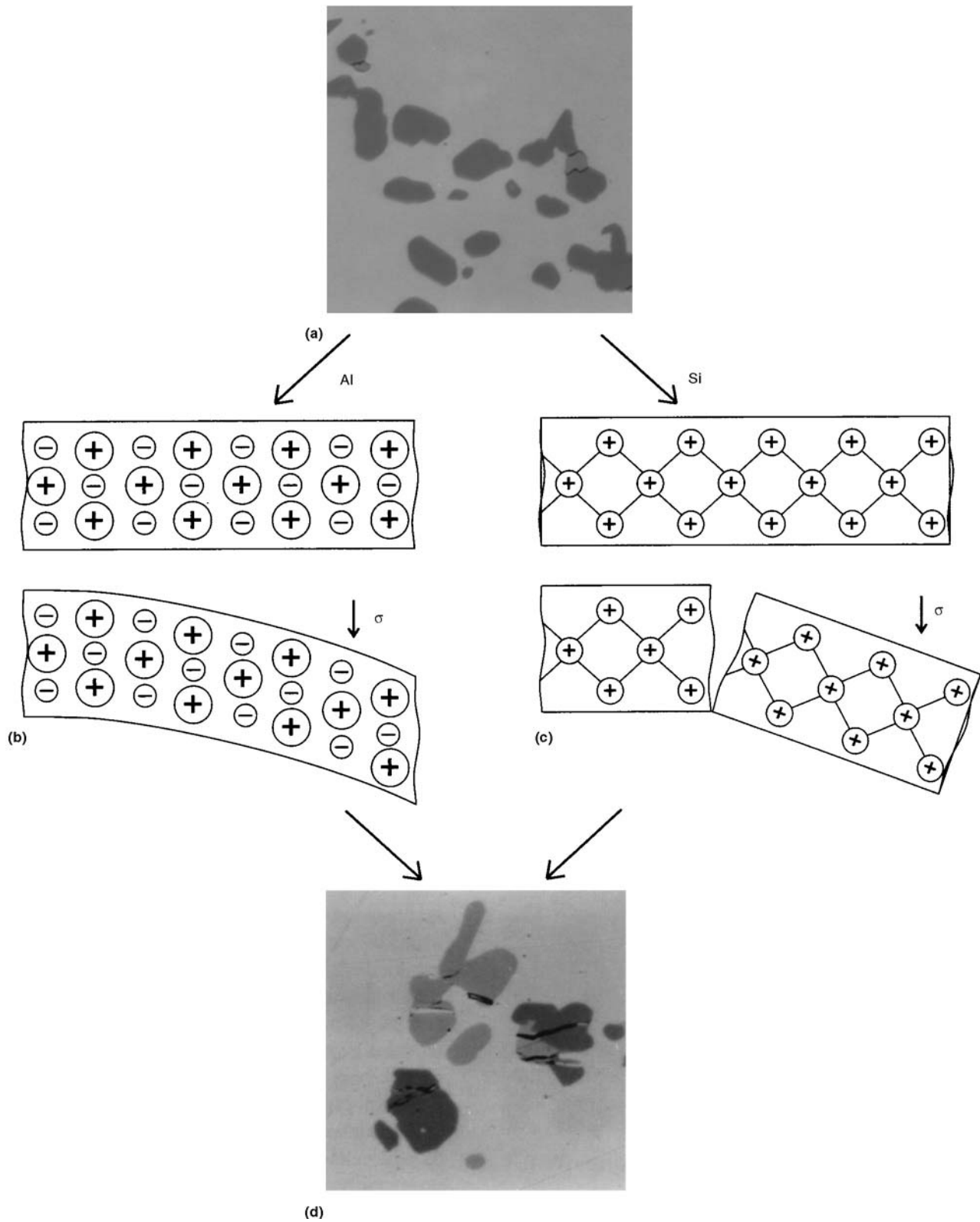


**Fig. 1.5** Properties of an aluminum-silicon alloy formed by its phase components. (a) Biphase microstructure of the aluminum-silicon brittle hard silicon particles in soft plastic aluminum matrix. (b) Reaction of the matrix under external loading (according to Ref 1). (c) Reaction of silicon particle under external loading (according to Ref 1). (d) Result of the loading of material

stituted atoms and vacancies or by precipitation hardening with dispersion particles of the second phase.

Decreasing the risk of brittle fracture in polyphase regions can be realized only by reducing the intensity of the stress-concentration effect on the silicon particles and by eliminating microregions of potential crack initiation. The breaking of the silicon precipitates network and their spheroidization are very important. This allows a decrease in the stress-concentration factor value in these regions, depending on brittle phase morphology (Ref 6, 14):

$$K_n = 2a/b \quad (\text{Eq 1.8})$$

where  $a$  is one-half the length of a particle and  $b$  is one-half the width of a particle.

Material of fine microstructure morphology has less tendency for low-energy brittle cracking. To obtain acceptable morphology and

degree of dispersion of the components, the foundry personnel can interfere at the crystallization stage by modifying the alloy and by controlling the solidification path and then, in the solid state, by heat treatment.

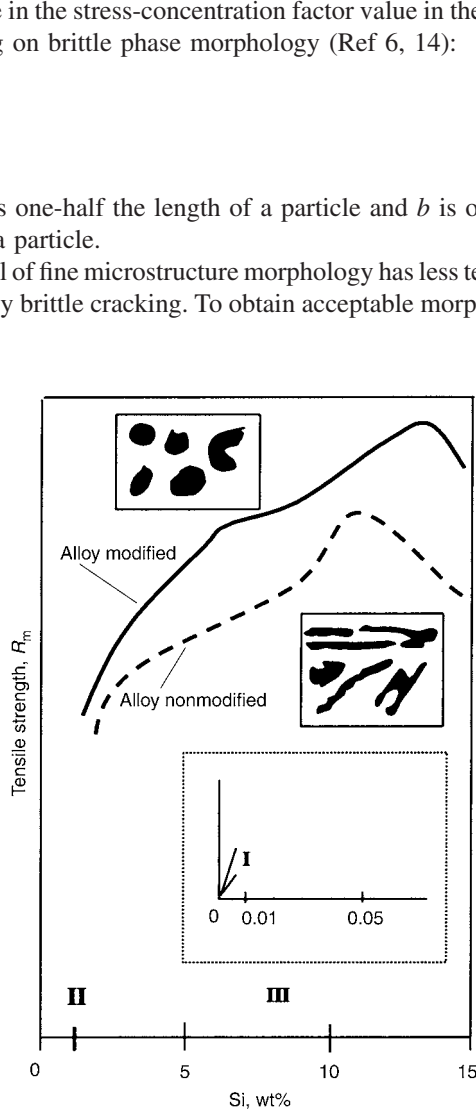


**Fig. 1.6** Tensile strength versus silicon content in aluminum-silicon cast alloy. Source: Ref 1

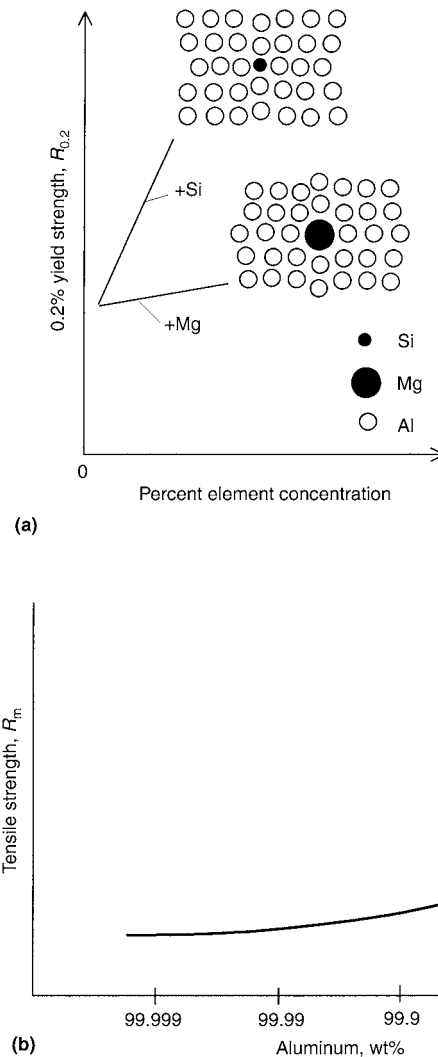


**Fig. 1.7** Influence of addition elements on mechanical properties of aluminum. (a) Deformation of crystal lattice caused by substitution atoms. (b) Change of the mechanical properties of  $\alpha$ -aluminum solid solution in presence of addition atoms. Source: Ref 1, 10

**Table 1.4** Properties of the alloying elements in aluminum-silicon commercial alloys

Element	Atomic number, $Z$	$M$	Crystal symmetry	Unit cell parameters		Atomic radius nm	Ion radius nm	Density g/cm <sup>3</sup>	Melting point, °C	Max. solubility in $\alpha$ -Al, wt%
				$\alpha$ , nm	$c$ , nm					
Mg	12	24.32	A3 hexagonal	0.320	0.520	0.160	0.066	1.74	650	14.9(450 °C)
Al	13	26.97	A1 cubic	0.4041	...	0.143	0.051	2.699	660.5	...
Si	14	28.06	A1 cubic	0.543	...	0.118	0.042	2.35	1440	1.65 (577 °C)
Mn	25	54.93	A1 cubic	0.893	...	0.112	0.080 <sup>(+2)</sup> 0.066 <sup>(+3)</sup>	7.43	1240	1.82 (660 °C)
Fe	26	55.84	Cubic	A1, 0.369 (916 °C) A2, 0.288 (20 °C)	...	A1, 0.124 A2, 0.127	A1, 0.064 A2, 0.074	7.87	1538	0.052 (655 °C)
Cu	29	63.57	A1 cubic	0.361	...	0.128	...	8.96	1083	5.67(550 °C)

Source: Ref 1, 3, 8–10

## 1.4 Effects of Different Levels of Silicon Contents

In the equilibrium diagram presented in Fig. 1.1 and in Fig. 1.6, several characteristic ranges of silicon content can be identified. In each range (I, II, III of Fig. 1.6), a different mechanism of the silicon influence on the properties of the alloy is present.

### 1.4.1 Silicon Contents of 0 to 0.01 wt%

In range I, silicon is substituted for aluminum atoms in solid solution. The silicon atoms situated in the nodes of crystallographic lattice strengthen the  $\alpha$ -aluminum solid solution (Table 1.4). Deformation of lattice caused by the difference in diameter of aluminum and silicon atoms makes the dislocations movement difficult. The atoms of other alloying elements can act in a similar manner. Even though their solubility in  $\alpha$ -aluminum solid solution is very small, trace quantities of alloying elements can change the mechanical properties of aluminum-silicon alloy to an important degree (Fig. 1.7) (Ref 1, 3, 10, 11). This is caused by very strong

interaction between either screw and edge dislocations and by the stress field introduced by the substitution atoms. Range of an introduced misfit in the hydrostatic stress field is directly proportional to the difference of atom radii between the matrix and the additional elements. The effect of the strengthening of  $\alpha$ -aluminum solid solution by the substitution of atoms of smaller radii than aluminum (such as silicon, manganese, iron, and copper) is more evident than in the case of atoms of larger radii (such as magnesium) (Fig. 1.7a). Some level of the strengthening can also be achieved owing to the nonsymmetric stress field around the disk vacancies, interacting with the nonsymmetric part of the stress field of either screw or edge dislocations (Table 1.3).

### 1.4.2 Silicon Contents of 0.01 to 1.65 wt%

In range II, a temperature-dependent terminal solid solution of silicon in aluminum forms can be strengthened by dispersed precipitation. During fast cooling  $\alpha$ -aluminum solid solution can be supersaturated and then, as a result of its tendency to achieve the thermodynamic equilibrium, the dispersed particles of silicon pre-

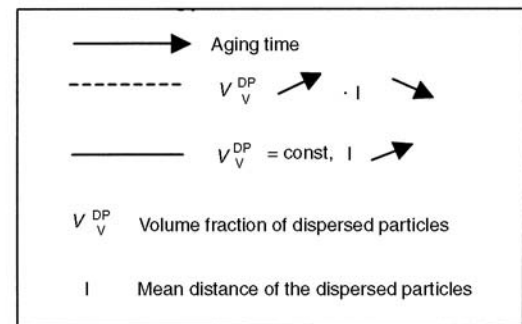
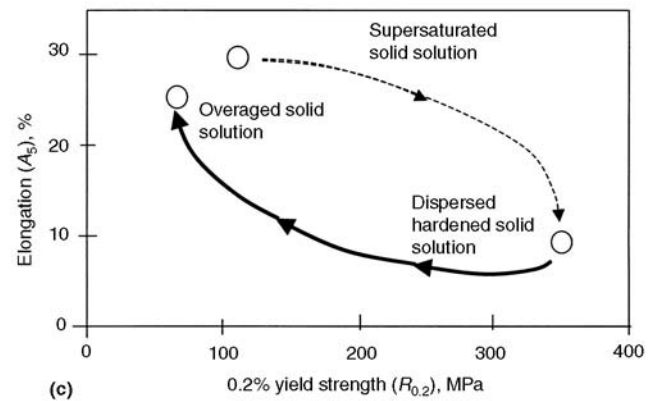
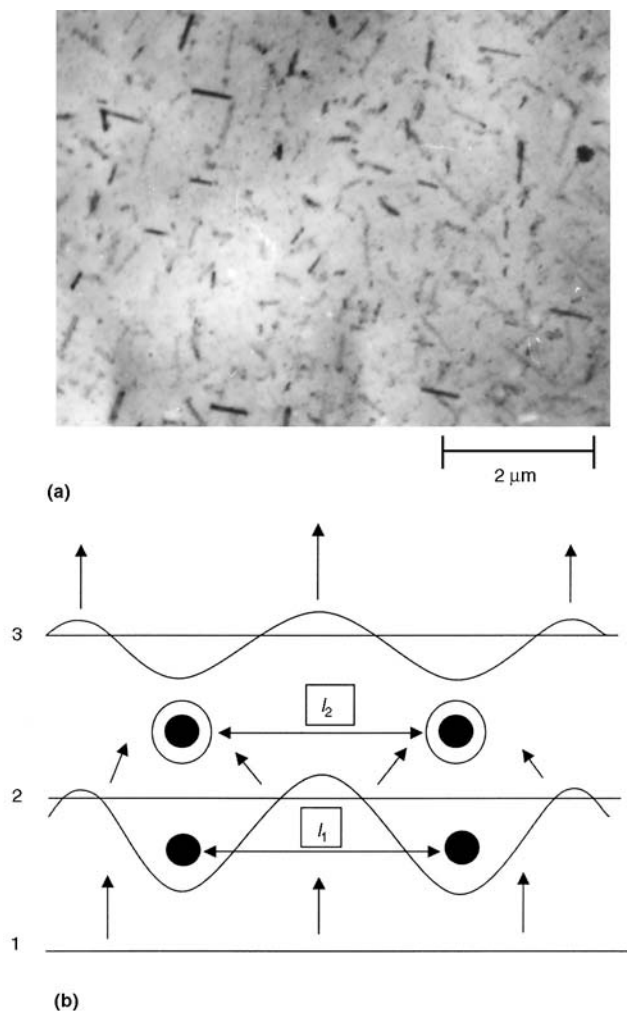


**Fig. 1.8** Precipitate hardening of the supersaturated  $\alpha$ -Al-solid solution. (a) Morphology of the disperse precipitates, C355-T6 alloy. TEM, 10,000 $\times$ . (b) Orowan mechanism—dislocation displacement in matrix with hard disperse particles. Areas labeled 1, 2, and 3 of (b) show successive steps of the process of displacement of the dislocation through material among dispersed precipitates.  $l_1$ , initial distance between precipitates.  $l_2$ , apparent distance when the first dislocation has gone through. (c) Change of material properties depending on the particles morphology. Source: Ref 1, 6, 12



precipitate on {111} and {100} planes (Ref 10). A similar event takes place in the presence of copper, manganese, and magnesium atoms. Dispersed particles of intermetallic phases can also precipitate from a supersaturated  $\alpha$ -aluminum solid solution. The material hardening with such particles can be explained taking into account an Orowan model (Fig. 1.8). Shear stress, which causes particle lateral dislocation, can be expressed by (Ref 5):

$$\tau = Gb/l \quad (\text{Eq 1.9})$$

where  $\tau$  is shear stress,  $G$  is shear modulus,  $b$  is Burgers vector, and  $l$  is the distance between dispersed particles.

As the distance between particles decreases and achieves some critical value, with simultaneous enlargement of their size, the stress necessary to move dislocations increases and material becomes hardened.

### 1.4.3 Silicon Contents Greater Than 1.65 wt%

In this silicon concentration range (III), the two-phase alloys solidify and the influence of silicon on properties can be described by Eq 1.3. Some misfits from linear dependence, visible in Fig. 1.6 (Ref 1), reflect the influence of morphology and distribution of silicon precipitates.

## REFERENCES

1. D.R. Askeland, *The Science and Engineering of Materials*, PWS-Kent Publishing Co., 1987
2. J. Massalski, *Fizyka dla inżynierów (Physics for Engineers)*, Vol 2, Wyd. Naukowo-Techniczne, Warsaw, 1976 (in Polish)
3. J.E. Hatch, Ed., *Aluminum: Properties and Physical Metallurgy*, American Society for Metals, 1984
4. M.F. Ashby, C. Ghandi, and M.R. Taplin, Fracture-Mechanism Maps and Their Construction for FCC Metals and Alloys, *Acta Metall.*, Vol 27, 1979, p 699–729
5. G.E. Dieter, *Mechanical Metallurgy*, 3rd ed., McGraw-Hill, 1986 p 241–271
6. R.W. Hertzberg, *Deformation and Fracture Mechanics of Engineering Materials*, John Wiley & Sons, 1989
7. M.L. Bernsztejn and W.A. Zajmowski, *Struktura i własności mechaniczne metali (Structure and Mechanical Properties of Metals)*, Wyd. Naukowo-Techniczne, Warsaw, 1973 (in Polish)
8. L. Kalinowski, *Fizyka metali (Physics of Metals)*, PWN, Warsaw, 1973 (in Polish)
9. C. Kittel, *Solid State Physics*, John Wiley & Sons, 1957
10. L.F. Mondolfo, *Aluminium Alloys: Structure and Properties*, Butterworths, London-Boston, 1976
11. Z. Poniewierski, *Krystalizacja, struktura i własności siluminów (Crystallization, Structure and Properties of Silumins)*, Wyd. Naukowo-Techniczne, Warsaw, 1989 (in Polish)
12. J.R. Davis, Ed., *ASM Specialty Handbook: Aluminum and Aluminum Alloys*, ASM International, 1993
13. S.-Z. Lu and A. Hellawell, Modification of Al-Si Alloys: Microstructure, Thermal Analysis and Mechanics, *JOM*, Vol 47 (No. 2), 1995, p 38–40
14. A. Gangulee and J. Gurland, On the Fracture of Silicon Particles in Al-Si Alloys, *Trans. Metall. Soc. AIME*, Vol 239 (No. 2), 1967, p 269–272
15. M.A. Przystupa and T.H. Courtney, Fracture in Equiaxed Two Phase Alloys: Part I. Fracture with Isolated Elastic Particles, *Metall. Trans. A*, Vol 13A (No. 5), 1982, p 873–879
16. H. Arbenz, Qualitätsbeschreibung von Aluminium—Guss-tücken Anhand von Gefügemerkmalen (The Use of Structural Features to Determine the Quality of Aluminum Castings), *Giesserei*, Vol 66 (No. 19), 1979, p 702–711 (in German)
17. C.H. Cáceres and Q.G. Wang, Dendrite Cell Size and Ductility of Al-Si-Mg Casting Alloys, *Int. J. Cast Metals Rev.*, Vol 9, 1996, p 157–162
18. O. Vorren, J.E. Evensen, and T.B. Pedersen, Microstructure and Mechanical Properties of AlSi(Mg) Casting Alloys, *AFS Trans.*, Vol 92, 1984, (84-462), p 549–466
19. H.M. Tensi and J. Hogerl, Metallographische Gefüge—Untersuchungen zur Qualitätssicherung von Al-Si Gussbau-teilen (Metallographic Investigation of Microstructure for Quality Assurance of Aluminum-Silicon Castings), *Metall*, Vol 48 (No. 10), 1994, p 776–781 (in German)
20. P.N. Crepeau, S.D. Antolovich, and J.A. Warden, Structure-Property Relationships in Aluminum Alloy 339-T5: Tensile Behavior at Room and Elevated Temperature, *AFS Trans.*, Vol 98, 1990, p 813–822



**ASM International** is the society for materials engineers and scientists, a worldwide network dedicated to advancing industry, technology, and applications of metals and materials.

ASM International, Materials Park, Ohio, USA  
[www.asminternational.org](http://www.asminternational.org)

This publication is copyright © ASM International®. All rights reserved.

Publication title	Product code
Aluminum-Silicon Casting Alloys: Atlas of Microfractographs	06993G

**To order products from ASM International:**

**Online** Visit [www.asminternational.org/bookstore](http://www.asminternational.org/bookstore)

**Telephone** 1-800-336-5152 (US) or 1-440-338-5151 (Outside US)

**Fax** 1-440-338-4634

**Mail** Customer Service, ASM International  
 9639 Kinsman Rd, Materials Park, Ohio 44073, USA

**Email** [CustomerService@asminternational.org](mailto:CustomerService@asminternational.org)

**In Europe** American Technical Publishers Ltd.  
 27-29 Knowl Piece, Wilbury Way, Hitchin Hertfordshire SG4 0SX, United Kingdom  
 Telephone: 01462 437933 (account holders), 01462 431525 (credit card)  
[www.ameritech.co.uk](http://www.ameritech.co.uk)

**In Japan** Neutrino Inc.  
 Takahashi Bldg., 44-3 Fuda 1-chome, Chofu-Shi, Tokyo 182 Japan  
 Telephone: 81 (0) 424 84 5550

**Terms of Use.** This publication is being made available in PDF format as a benefit to members and customers of ASM International. You may download and print a copy of this publication for your personal use only. Other use and distribution is prohibited without the express written permission of ASM International.

No warranties, express or implied, including, without limitation, warranties of merchantability or fitness for a particular purpose, are given in connection with this publication. Although this information is believed to be accurate by ASM, ASM cannot guarantee that favorable results will be obtained from the use of this publication alone. This publication is intended for use by persons having technical skill, at their sole discretion and risk. Since the conditions of product or material use are outside of ASM's control, ASM assumes no liability or obligation in connection with any use of this information. As with any material, evaluation of the material under end-use conditions prior to specification is essential. Therefore, specific testing under actual conditions is recommended.

Nothing contained in this publication shall be construed as a grant of any right of manufacture, sale, use, or reproduction, in connection with any method, process, apparatus, product, composition, or system, whether or not covered by letters patent, copyright, or trademark, and nothing contained in this publication shall be construed as a defense against any alleged infringement of letters patent, copyright, or trademark, or as a defense against liability for such infringement.